

Absolute Binding Energies of Sodium Ions to Short Chain Alcohols, $C_nH_{2n+2}O$, $n = 1-4$, Determined by Threshold Collision-Induced Dissociation Experiments and Ab Initio Theory

M. T. Rodgers*

Department of Chemistry, Wayne State University, Detroit, Michigan 48202

P. B. Armentrout*

Department of Chemistry, University of Utah, Salt Lake City, Utah 84112

Received: February 23, 1999; In Final Form: April 28, 1999

Collision-induced dissociation of $Na^+(ROH)$ with xenon is studied using guided ion beam mass spectrometry. ROH includes the following eight short chain alcohols: methanol, ethanol, 1-propanol, 2-propanol, *n*-butyl alcohol, isobutyl alcohol, sec-butyl alcohol, and *tert*-butyl alcohol. In all cases, the primary product formed corresponds to endothermic loss of the neutral alcohol. The only other products that are observed in these reactions are the result of ligand exchange processes to form $NaXe^+$. The cross section thresholds are interpreted to yield 0 and 298 K bond energies for Na^+-ROH after accounting for the effects of multiple ion–molecule collisions, internal energy of the reactant ions, and dissociation lifetimes. Ab initio calculations at several levels of theory compare favorably to the experimentally determined bond energies. Trends in the Na^+ binding energies are also compared to experimental values for the analogous Li^+ systems.

Introduction

In recent work, we have developed methods to allow the application of quantitative threshold collision-induced dissociation methods to obtain accurate thermodynamic information on increasingly large systems.^{1–4} The major driving force behind these developments is our interest in applying such techniques to systems of biological relevance. Noncovalent metal–ligand interactions play a primary role in determining the structure and function in biological molecules. Quantitative studies in the gas phase provide one way of obtaining more detailed information on such effects because the individual interactions can be easily isolated. In the present study, we examine a simple metal–ligand system that can act as a fundamental model for noncovalent metal–ligand interactions: $Na^+(ROH)$, where ROH = methanol (MeOH), ethanol (EtOH), 1-propanol (1-PrOH), 2-propanol (2-PrOH), *n*-butyl alcohol (*n*-BuOH), isobutyl alcohol (*i*-BuOH), sec-butyl alcohol (*s*-BuOH), and *tert*-butyl alcohol (*t*-BuOH). In addition, these systems form an intrinsically interesting sequence in which the size and geometry of the alkyl group provide a systematic influence on the binding energies.

In this work, we directly measure the absolute bond dissociation energies (BDEs) of the $Na^+(ROH)$ species using guided ion beam mass spectrometry. For all but the methanol and 2-propanol systems, these constitute the first experimental determinations of these BDEs. Trends in the values are directly compared to those previously measured in our laboratory for the analogous Li^+ complexes.² In addition, theoretical calculations at the RHF/6-31G** and MP2(full)/6-31G* levels are carried out to provide structures, vibrational frequencies, and rotational constants needed for the analysis of the data. The present experimental results are compared to binding energies calculated at the MP2(full)/6-311+G(2d,2p) level, including corrections for basis set superposition errors and using G2 theory⁵ and the complete basis set extrapolation protocols, CBS-4 and CBS-Q.^{6,7}

Experimental and Computational Section

General Experimental Procedures. Cross sections for CID of sodiated alcohols are measured using a guided ion beam mass spectrometer that has been described in detail previously.^{8,9} The metal ligand complexes are generated as described below. The ions are extracted from the source, accelerated, and focused into a magnetic sector momentum analyzer for mass analysis. Mass-selected ions are decelerated to a desired kinetic energy and focused into an octopole ion guide, which traps the ions in the radial direction.¹⁰ The octopole passes through a static gas cell containing xenon, used as the collision gas, for reasons described elsewhere.^{11–13} Low gas pressures in the cell (typically 0.05–0.20 mTorr) are used to ensure that multiple ion–molecule collisions are improbable. Product and unreacted beam ions drift to the end of the octopole, where they are focused into a quadrupole mass filter for mass analysis and subsequently detected with a secondary electron scintillation detector and standard pulse counting techniques.

Ion intensities are converted to absolute cross sections as described previously.⁸ Absolute uncertainties in cross section magnitudes are estimated to be $\pm 20\%$, which are largely the result of error in the pressure measurement and the length of the interaction region. Ion kinetic energies in the laboratory frame, E_{lab} , are converted to energies in the center of mass frame, E_{CM} , using the formula $E_{CM} = E_{lab}m/(m + M)$, where M and m are the masses of the ionic and neutral reactants, respectively. All energies reported below are in the CM frame unless otherwise noted. The absolute zero and distribution of the ion kinetic energies are determined using the octopole ion guide as a retarding potential analyzer as previously described.⁸ Because the reaction zone and energy analysis region are physically the same, ambiguities in the energy analysis resulting from contact potentials, space charge effects, and focusing aberrations are minimized.⁸ The distribution of ion kinetic energies is nearly Gaussian with a fwhm typically between 0.2 and 0.3 eV (lab)

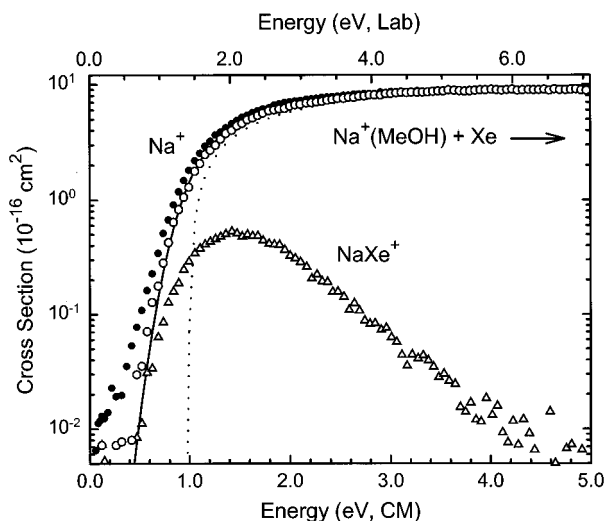


Figure 1. Cross sections for collision-induced dissociation of $\text{Na}^+(\text{MeOH})$ with Xe as a function of kinetic energy in the center-of-mass frame (lower x axis) and the laboratory frame (upper x axis). Data are shown for a xenon pressure of 0.18 mTorr (closed circles) and extrapolated to zero (open circles). Cross sections for the ligand exchange process to form NaXe^+ are shown by open triangles. The solid line shows the best fit to the data using the model of eq 1 convoluted over the neutral and ion kinetic and internal energy distributions. The dotted line shows the model cross section in the absence of experimental kinetic energy broadening for reactants with an internal energy of 0 K.

for these experiments. The uncertainty in the absolute energy scale is ± 0.05 eV (lab).

Even when the pressure of the reactant neutral is low, we have previously demonstrated that the effects of multiple collisions can significantly influence the shape of CID cross sections.¹⁴ Because the presence and magnitude of these pressure effects is difficult to predict, we have performed pressure dependent studies of all cross sections examined here. In the present systems, we observe small cross sections at low energies that have an obvious dependence upon pressure. This is illustrated in Figure 1. We attribute this to multiple energizing collisions that lead to an enhanced probability of dissociation below threshold as a result of the longer residence time of these slower moving ions. Data free from pressure effects are obtained by extrapolating to zero reactant pressure, as described previously.¹⁴ Thus, results reported below are due to single bimolecular encounters.

Ion Source. The $\text{Na}^+(\text{ROH})$ complexes are formed in a 1 m long flow tube^{9,15} operating at a pressure of 0.5–0.7 Torr with a helium flow rate of about 6000 sccm. Sodium ions are generated in a continuous dc discharge by argon ion sputtering of a cathode, made from tantalum, with a cavity containing sodium metal. Typical operating conditions of the discharge are about 1.4–1.8 kV and 20–30 mA in a flow of roughly 10% argon in helium. The $\text{Na}^+(\text{ROH})$ complexes are formed by associative reactions of the sodium ion with a neutral alcohol that is introduced into the flow 50 cm downstream from the dc discharge. The flow conditions used in this ion source provide in excess of 10^4 collisions between an ion and the buffer gas, which should thermalize the ions both vibrationally and rotationally. In our analysis of the data, we assume that the ions produced in this source are in their ground electronic states and that the internal energy of the $\text{Na}^+(\text{ROH})$ complexes is well-described by a Maxwell–Boltzmann distribution of ro-vibrational states at 300 K. Previous work from this laboratory has shown that these assumptions are generally valid.^{14–20}

Thermochemical Analysis. The threshold regions of the reaction cross sections are modeled using eq 1

$$\sigma(E) = \sigma_0 \sum_i g_i (E + E_i - E_0)^n / E \quad (1)$$

where σ_0 is an energy independent scaling factor, E is the relative translational energy of the reactants, E_0 is the threshold for reaction of the ground electronic and ro-vibrational state, and n is an adjustable parameter. The summation is over the ro-vibrational states of the reactant ions, i , where E_i is the excitation energy of each state and g_i is the population of those states ($\sum g_i = 1$). The populations of excited ro-vibrational levels are not negligible even at 300 K as a result of the many low-frequency modes present in these ions. The relative reactivities of all ro-vibrational states, as reflected by σ_0 and n , are assumed to be equivalent. Vibrational frequencies and rotational constants are taken from ab initio calculations (RHF/6-31G** values scaled by 0.9) as detailed in the next section. The Beyer–Swinehart algorithm²¹ is used to evaluate the density of the ro-vibrational states, and the relative populations g_i are calculated by an appropriate Maxwell–Boltzmann distribution at the 300 K temperature appropriate for the reactants. We have estimated the sensitivity of our analysis to the deviations from the true frequencies by scaling the calculated RHF/6-31G** frequencies to encompass the range of average valence coordinate scale factors needed to bring calculated frequencies into agreement with experimentally determined frequencies found by Pople et al.²² Thus, the originally calculated vibrational frequencies were scaled by 0.7 and 1.1. The corresponding changes in the data analysis are included in the uncertainties listed with the values and other fitting parameters.

We also consider the possibility that collisionally activated complex ions do not dissociate on the time scale of our experiment (about 10^{-4} s) by including statistical theories for unimolecular dissociation into eq 1 as described in detail elsewhere.^{2,17} This requires sets of ro-vibrational frequencies appropriate for the energized molecules and the transition states (TSs) leading to dissociation. We assume that the TSs are loose and productlike because the interaction between the sodium ion and the alcohol is largely electrostatic. In this case, the TS vibrations used are the frequencies corresponding to the products, which were also calculated as detailed below. The transitional frequencies, those that become rotations of the completely dissociated products, are treated as rotors, a treatment that corresponds to a phase space limit (PSL) and is described in detail elsewhere.³ For the $\text{Na}^+(\text{ROH})$ complexes, the two transitional mode rotors have rotational constants equal to those of the neutral alcohol product with axes perpendicular to the reaction coordinate. The external rotations of the energized molecule and TS are also included in the modeling of the CID data. The external rotational constants of the TS are determined by assuming that the TS occurs at the centrifugal barrier for interaction of Na^+ with the neutral alcohol, calculated variationally as outlined elsewhere.³ The 2-D external rotations are treated adiabatically but with centrifugal effects included consistent with the discussion of Waage and Rabinovitch.²³ In the present work, the adiabatic 2-D rotational energy is treated using a statistical distribution with explicit summation over the possible values of the rotational quantum number, as described in detail elsewhere.³

The model represented by eq 1 is expected to be appropriate for translationally driven reactions²⁴ and has been found to reproduce reaction cross sections well in a number of previous studies of both atom–diatom and polyatomic reactions,^{13,25} including CID processes.^{1–3,14–17,26} The model is convoluted

with the kinetic energy distributions of both reactants, and a nonlinear least-squares analysis of the data is performed to give optimized values for the parameters σ_0 , E_0 , and n . The error associated with the measurement of E_0 is estimated from the range of threshold values determined for different data sets, variations associated with uncertainties in the vibrational frequencies, and the error in the absolute energy scale, 0.05 eV (lab). For analyses that include the RRKM lifetime effect, the uncertainties in the reported E_0 values also include the effects of increasing and decreasing the time assumed available for dissociation (10^{-4} s) by a factor of 2.

Equation 1 explicitly includes the internal energy of the ion, E_i . All energy available is treated statistically, which should be a reasonable assumption because the internal (rotational and vibrational) energy of the reactants is redistributed throughout the ion upon impact with the collision gas. The threshold for dissociation is by definition the minimum energy required for dissociation and thus corresponds to formation of products with no internal excitation. The assumption that products formed at threshold have an internal temperature of 0 K has been tested for several systems.^{1,2,14–17} It has been shown that treating all energy of the ion (vibrational, rotational, and translational) as capable of coupling into the dissociation coordinate leads to reasonable thermochemistry. The threshold energies for dissociation reactions determined by analysis with eq 1 are converted to 0 K bond energies by assuming that E_0 represents the energy difference between reactants and products at 0 K.²⁷ This requires that there are no activation barriers in excess of the endothermicity of dissociation. This is generally true for ion–molecule reactions²⁷ and should be valid for the simple heterolytic bond fission reactions examined here.²⁸

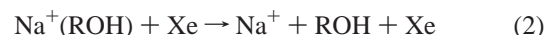
Computational Details. To obtain model structures, vibrational frequencies, and energetics for the neutral and sodiated alcohols, ab initio calculations were performed with the Hyperchem software package²⁹ and then refined at higher levels of theory using Gaussian 98W.³⁰ In all calculations, the starting structures are annealed and then energy minimized at low levels of theory (semiempirical, RHF/STO-3G, RHF/3-21G, and RHF/6-31G** using Hyperchem) to obtain good starting structures for the final geometry optimization calculations performed at the MP2(full)/6-31G* level.^{31–33} This level of theory was recently determined by Hoyau et al. to be adequate for a good description of sodium cation complexes.³⁴ Several conformers of both the free and sodiated alcohols were included in these calculations. Vibrational analyses of the geometry-optimized structures were performed to determine the vibrational frequencies and rotational constants of the molecules. Such constants were obtained at both the RHF/6-31G** and MP2(full)/6-31G* levels, and the latter values are listed in Tables 1S and 2S, available as Supporting Information. When used to model the data or to calculate thermal energy corrections, the MP2(full)/6-31G* vibrational frequencies are scaled by a factor of 0.9646,^{15,35} while the RHF/6-31G** frequencies are scaled by 0.9, as suggested by recent work.³⁶ For historical reasons, most of the data analysis was conducted with the RHF/6-31G** molecular constants, but it was verified that the use of the MP2(full)/6-31G* constants yielded nearly identical results (deviations in E_0 values were less than 0.01 eV). All thermal energy corrections were obtained using the scaled MP2(full)/6-31G* frequencies.

Single point energy calculations were performed at the MP2(full)/6-311+G(2d,2p) level using the MP2(full)/6-31G* geometries. To obtain accurate bond dissociation energies for the MP2 calculations, basis set superposition errors (BSSE) were subtracted from the computed dissociation energies in the full

counterpoise approximation,^{37,38} as in several other recent papers on Na⁺ complexes.^{34,39,40} The BSSE corrections ranged from 4.8 kJ/mol for Na⁺(MeOH) to about 8 kJ/mol for the Na⁺-(butanol) complexes. To check the accuracy of these theoretical predictions, we also carried out complete basis set extrapolations at the CBS-4 and CBS-Q levels of theory^{6,7} for all eight Na⁺-(ROH) complexes. The CBS-4 model theory includes corrections for higher order correlation effects calculated at the MP4 level with a modest sized basis set (6-31G), but may be limited by the geometry optimization which is conducted at the HF/3-21G* level. The CBS-Q calculations determine geometries at the MP2(FC)/6-31G⁺ level and include higher order correlation corrections at the MP4 and QCISD(T) levels of theory. For the four smallest complexes (excluding the butanol systems), we also carried out G2 calculations⁵ which determine geometries at the MP2(full)/6-31G* level and again include higher order correlation corrections at the MP4 and QCISD(T) levels of theory. All these calculations were carried out using the Gaussian 98W³⁰ suite of programs.

Results

Cross Sections for Collision-Induced Dissociation. Experimental cross sections were obtained for the interaction of Xe with eight Na⁺(ROH) complexes, where ROH = methanol, ethanol, 1-propanol, 2-propanol, *n*-butyl alcohol, isobutyl alcohol, sec-butyl alcohol, and *tert*-butyl alcohol. Figure 1 shows representative data for the Na⁺(MeOH) system. A complete set of figures for all eight systems examined can be obtained from Figure 1S of the Supporting Information. The most favorable process observed for all complexes is the loss of the intact ligand in the collision-induced dissociation (CID) reaction 2.



The magnitudes of the cross sections increase slightly as the size of the alcohol increases. The only other product observed in these reactions⁴¹ is the result of ligand exchange processes to form NaXe⁺. This is shown in Figure 1, the case where this product is the largest. For the other seven systems, the maximum cross sections for the NaXe⁺ product are about 2 orders of magnitude smaller than those for the primary Na⁺ product. In all cases, thresholds for NaXe⁺ are slightly lower than for Na⁺ (by the Na⁺–Xe binding energy). As little systematic information can be gleaned from these products, they will not be discussed further. However, it is conceivable that this ligand exchange process might cause a competitive shift in the observed thresholds, at least in the case of the methanol system. We do not believe such competition is likely to affect our threshold measurements in any of these systems for several reasons that have been detailed elsewhere.⁴² In the present case, we also note that a competitive shift would make the true threshold for dissociation of Na⁺(MeOH) even lower than the number presently reported. As is evident from the discussion below, such a result is almost certainly incorrect.

Threshold Analysis. The model of eq 1 was used to analyze the thresholds for reaction 2 in eight Na⁺(ROH) systems. The results of these analyses are provided in Table 1 and shown in Figure 2 for representative examples of two primary alcohols, one small (methanol) and one large (*n*-butyl alcohol); one secondary alcohol (2-propanol); and the tertiary alcohol (*tert*-butyl alcohol). A complete set of figures for all eight systems examined can be obtained as Figure 2S of the Supporting Information. The experimental cross sections for reaction 2 in all eight systems are accurately reproduced using a loose phase

TABLE 1: Threshold Dissociation Energies at 0 K and Entropies of Activation at 1000 K of Na⁺(ROH)^a

reactant complex	σ_0^b	n^b	E_0^c (eV)	$E_0(\text{PSL})$ (eV)	$\Delta S^\ddagger(\text{PSL})$ (J mol ⁻¹ K ⁻¹)
Na ⁺ (MeOH)	11.5(0.2)	1.1(0.1)	0.95(0.06)	0.95(0.06)	22(5)
Na ⁺ (EtOH)	13.9(0.4)	1.1(0.1)	1.06(0.04)	1.06(0.04)	26(5)
Na ⁺ (1-PrOH)	16.1(0.4)	1.1(0.1)	1.13(0.04)	1.12(0.04)	29(5)
Na ⁺ (2-PrOH)	14.9(1.3)	1.1(0.1)	1.18(0.05)	1.17(0.05)	33(5)
Na ⁺ (<i>n</i> -BuOH)	21.5(1.5)	1.1(0.1)	1.16(0.05)	1.13(0.05)	26(5)
Na ⁺ (<i>i</i> -BuOH)	15.7(1.8)	1.2(0.1)	1.14(0.06)	1.09(0.06)	32(5)
Na ⁺ (<i>s</i> -BuOH)	18.0(0.7)	1.1(0.1)	1.28(0.06)	1.22(0.05)	30(5)
Na ⁺ (<i>t</i> -BuOH)	13.0(0.8)	1.3(0.1)	1.24(0.04)	1.21(0.04)	30(5)

^a Uncertainties are listed in parentheses. ^b Average values for loose PSL transition state. ^c No RRKM analysis.

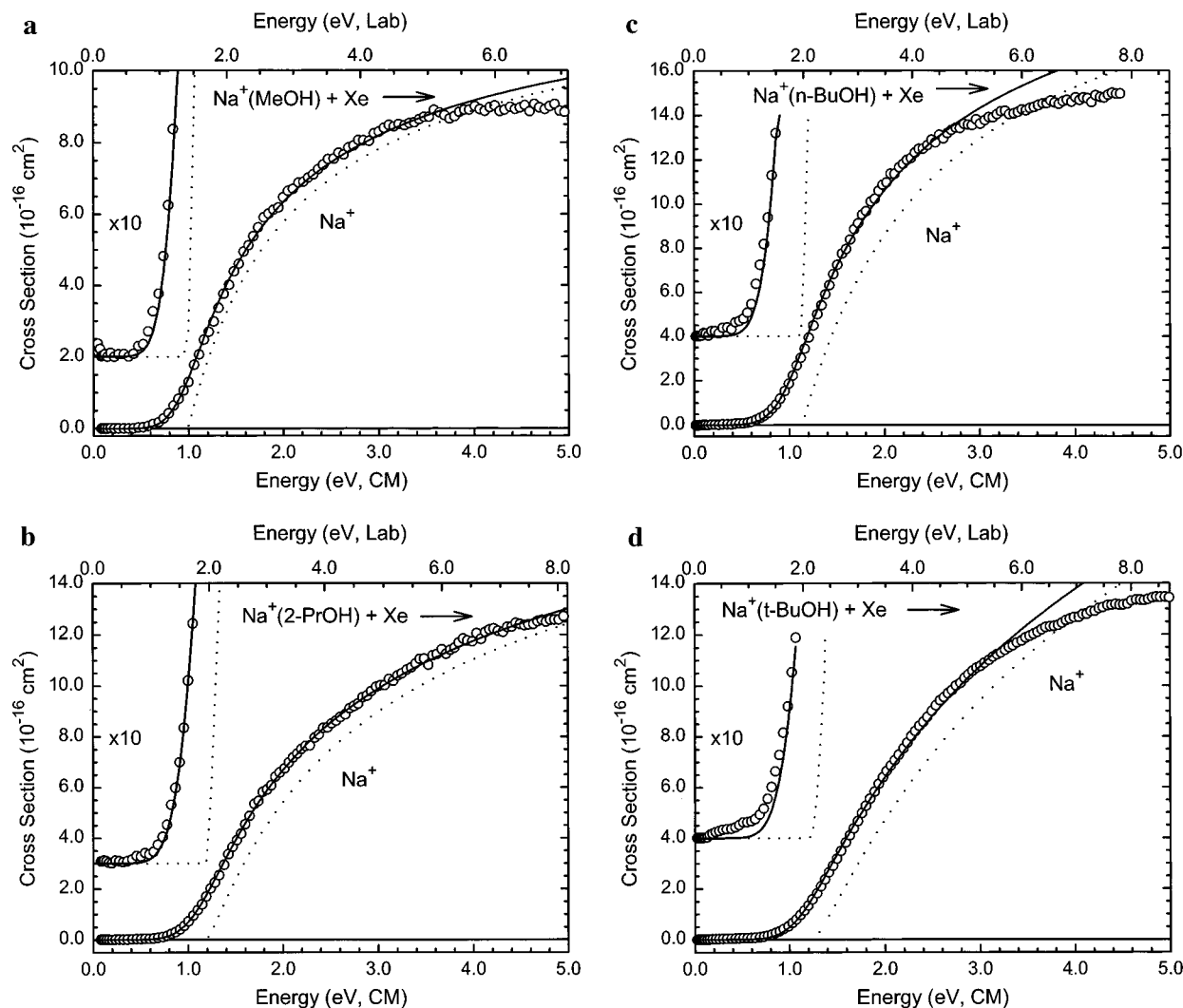


Figure 2. Zero pressure extrapolated cross sections for collision-induced dissociation of Na⁺(ROH) complexes where ROH = methanol, 2-propanol, *n*-butyl alcohol, *tert*-butyl alcohol (parts a–d, respectively) with Xe in the threshold region as a function of kinetic energy in the center-of-mass frame (lower x axis) and the laboratory frame (upper x axis). Solid lines show the best fits to the data using the model of eq 1 convoluted over the neutral and ion kinetic and internal energy distributions. Dotted lines show the model cross sections in the absence of experimental kinetic energy broadening for reactants with an internal energy of 0 K.

space limit (PSL) TS model.³ Previous work has shown that this model provides the most accurate assessment of the kinetic shifts for CID processes.^{1–3,26,42} Good reproduction of the data is obtained over energy ranges exceeding 2 eV (4 eV for the methanol, ethanol, 1-propanol, and 2-propanol systems) and cross section magnitudes of at least a factor of 100. Figure 2 shows that there are small “tails” at low energies in the data for the butanols. The data analysis is insensitive to these tails because of their extremely small size.

Table 1 also includes values of E_0 obtained without including the RRKM lifetime analysis. Comparison of these values with the $E_0(\text{PSL})$ values shows that the kinetic shifts are small in all

cases, but vary with the size and geometry of the alcohol. Dissociation of Na⁺(MeOH) and Na⁺(EtOH) show no kinetic shifts. As the size of the alcohol increases, the kinetic shift gradually increases, reaching a maximum for Na⁺(*s*-BuOH), which exhibits a kinetic shift of 0.065 eV. This is reasonable because the Na⁺(MeOH) system has only three heavy atoms and 15 vibrational modes, while the butanol systems have six heavy atoms and 42 vibrational modes. Kinetic shifts vary among the butanol systems (from 0.026 to 0.065 eV) because they depend on the dissociation energy (higher E_0 values lead to larger kinetic shifts) and TS geometries. The latter are reflected by the entropies of activation, ΔS^\ddagger , a measure of the

TABLE 2: MP2(full)/6-31G* Geometry Optimized Structures of the Neutral and Sodiated Alcohols

species	E_{rel} (kJ/mol)	bond length (Å)				bond angle (deg)		
		H—O	O—C	Na ⁺ —O	Na ⁺ —C _ω ^a	HOC	NaOC	ONaC _ω ^a
methanol		0.970	1.423			107.4		
Na ⁺ (MeOH)		0.973	1.454	2.209		107.3	129.3	
ethanol		0.972	1.427			107.1		
Na ⁺ (EtOH)		0.974	1.457	2.203	3.069 (β)	108.5	120.9	45.5 (β)
1-propanol		0.972	1.426			106.9		
Na ⁺ (1-PrOH)	0.0	0.974	1.455	2.202	3.011 (β)	108.7	118.6	46.4 (β)
	2.0	0.974	1.456	2.204	3.080 (β), 3.125(γ)	108.4	120.4	45.3 (β), 42.0 (γ)
2-propanol		0.973	1.432			107.3		
Na ⁺ (2-PrOH)		0.975	1.465	2.198	3.028 (β)	108.1	120.8	46.1 (β)
<i>n</i> -butyl alcohol		0.971	1.428			107.7		
Na ⁺ (<i>n</i> -BuOH)	0.0	0.974	1.456	2.202	2.969 (β)	108.8	117.3	47.0 (β)
	1.1	0.974	1.459	2.210	2.811 (δ)	107.6	124.7	59.5 (δ)
	1.6	0.974	1.456	2.203	3.043 (β), 3.089 (γ)	108.5	119.3	45.9 (β), 42.2 (γ)
isobutyl alcohol		0.971	1.428			107.7		
Na ⁺ (<i>i</i> -BuOH)	0.0	0.974	1.455	2.205	3.050 (β), 3.078 (γ)	108.5	118.8	45.8 (β), 42.7 (γ)
	2.6	0.973	1.458	2.213	3.024 (γ)	108.3	116.4	43.7 (γ)
sec-butyl alcohol		0.973	1.433			107.4		
Na ⁺ (<i>s</i> -BuOH)	0.0	0.975	1.465	2.199	2.980 (β)	108.2	119.4	46.8 (β)
	1.3	0.975	1.465	2.199	3.050 (β), 3.089 (γ)	108.0	120.6	45.7 (β), 42.4(γ)
<i>tert</i> -butyl alcohol		0.974	1.438			106.9		
Na ⁺ (<i>t</i> -BuOH)		0.975	1.475	2.191	2.999 (β)	107.6	120.9	46.4 (β)

^a ω refers to the carbon atom closest to the sodium cation.

looseness of the TS. Listed in Table 1 at 1000 K, these entropies of activation can be favorably compared to $\Delta S^{\ddagger}_{1000}$ values in the range 29–46 J mol⁻¹ K⁻¹ collected by Lifshitz for several simple bond cleavage dissociations of ions.⁴³ This is reasonable, considering that the TS is expected to lie at the centrifugal barrier for association of Na⁺ + ROH.

Theoretical Results. Structures for the eight neutral alcohols and for the complexes of all these species with Na⁺ were calculated as described above. Table 2 gives details of the final geometries for each of these species along with values for several low-lying conformations as well. Results for the most stable conformations of the sodium ion–alcohol complexes are shown in Figure 3. Not surprisingly, the calculations find that the sodium ion prefers to be bound to the oxygen atoms for all alcohols. The distortion of the alcohol upon sodium ion binding is small although the O–C bond length increases by about 0.03 Å and the HOC bond angle increases by about 1°. As in the case of the Li⁺(ROH) complexes, we find that the alkyl chain ligates the metal cation center as well.² This is indicated in Table 2 by the Na⁺–C_ω bond length and NaOC_ω bond angle, where C_ω indicates the carbon found closest to the sodium center. For most systems, the lowest energy conformer has the β carbon about 3 Å away from the sodium. The Na⁺(EtOH) system is prototypical in this regard. When the alkyl chain is longer, there is the possibility of additional conformers in which both the β and γ carbons are fairly close to the metal center. Such conformers were identified as stationary points for the 1-propanol, *n*-butyl alcohol, isobutyl alcohol, and sec-butyl alcohol systems. This is calculated to be the ground state conformer in the isobutyl alcohol system, which also has a low energy conformer in which the γ carbon is oriented to give a slightly shorter distance to Na⁺. Likewise, the *n*-butyl alcohol system has a low-energy conformer in which the δ carbon wraps around to give a relatively short Na⁺–C_δ distance of 2.811 Å. The three conformers for the *n*-butyl alcohol system are compared in Figure 4.

Sodium ion binding energies were determined using the MP2-(full)/6-31G* geometries and single point energy calculations performed at the MP2(full)/6-311+G(2d,2p) level. MP2 values corrected for zero point energies and BSSE are listed in Table 3 for the most stable conformer and low-lying conformers in the cases of alcohols having alkyl chains of three carbons or more.

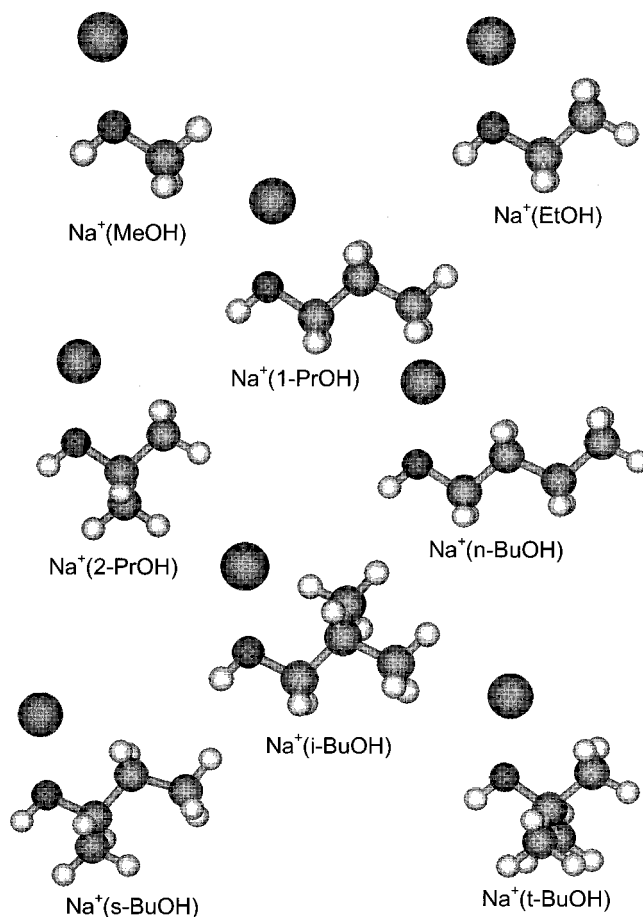


Figure 3. Ground-state geometries of Na⁺(ROH) where ROH = methanol, ethanol, 1-propanol, 2-propanol, *n*-butyl alcohol, isobutyl alcohol, sec-butyl alcohol, and *tert*-butyl alcohol optimized at the MP2-(full)/6-31G* level of theory.

In all cases, the energies of these alternate conformers are 1–3 kJ/mol higher than the most stable conformer. For comparison, this table also lists dissociation energies calculated for the most stable conformers of all eight alcohol complexes using the complete basis set extrapolation protocols, CBS-4 and CBS-

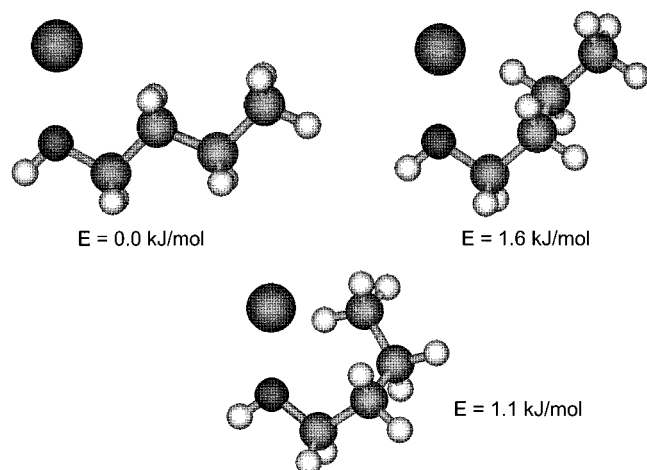


Figure 4. Ground and excited state conformations of $\text{Na}^+(\text{n-BuOH})$ calculated at the MP2(full)/6-31G* level of theory.

TABLE 3: Experimental and Calculated Enthalpies of Sodium Ion Binding of ROH in kJ/mol

complex	ΔH_0 (expt)	ΔH_0^a (calc)			
		MP2 ^a	CBS-4 ^b	CBS-Q ^b	G2 ^c
$\text{Na}^+(\text{MeOH})$	91.7(5.7)	100.0	92.9	96.2	98.5
$\text{Na}^+(\text{EtOH})$	102.0(3.7)	108.9	101.0	104.4	107.6
$\text{Na}^+(\text{1-prOH})$	108.0(4.1)	112.0	104.3	108.7	103.0
		110.0		108.4	
$\text{Na}^+(\text{2-prOH})$	113.2(4.3)	113.0	105.4	117.0	103.7
$\text{Na}^+(\text{n-BuOH})$	109.4(4.7)	114.5	109.8	109.4	
		113.4			
		112.9			
$\text{Na}^+(\text{i-BuOH})$	105.2(5.7)	112.6	106.1	115.2	
		110.0			
$\text{Na}^+(\text{s-BuOH})$	117.2(5.1)	117.1	109.6	118.9	
		115.8			
$\text{Na}^+(\text{t-BuOH})$	116.5(4.1)	116.8	109.5	113.5	

^a Calculated using MP2(full)/6-311+G(2d,2p)//MP2(full)/6-31G* (energy//geometry and frequencies) corrected for basis-set superposition error. ^b Calculated using the complete basis set extrapolation methods (CBS-4 or CBS-Q) outlined in refs 6 and 7. ^c Calculated using the G2 method outlined in ref 5.

Q,⁷ and the G2 method⁵ for the smallest complexes (no BSSE corrections were applied in these cases). These three methods have been found to have mean average deviations (MAD) of 8.4, 4.2, and 5.0 kJ/mol, respectively, for the G2 test set of thermodynamic values.³⁵ G2 calculations on butanol complexes were beyond our resources. We find that the CBS-4 bond energies are systematically lower than the MP2 values by an average of 7.3 ± 0.5 kJ/mol. For the methanol and ethanol complexes, the G2 and CBS-Q results lie between the higher MP2 values and the lower CBS-4 values, while for the propanol complexes, G2 theory gives the lowest bond energies of any theory (indeed lower than the G2 value for the ethanol complex). For larger clusters, there are no systematic trends in the relative numbers. In most cases, the highest (often MP2) and lowest (often CBS-4) theoretical values span a range of about 8 kJ/mol.

Discussion

As expected, the bond energies increase with increasing size of the alcohol. As the bonding is largely electrostatic, the dipole moments and polarizabilities of the alcohols must be considered in understanding this trend. Because there is little variation in the dipole moments of the alcohols (less than 5% differences) and methanol has the largest permanent dipole,⁴⁴ it seems clear that the observed trend is largely an effect of the increasing

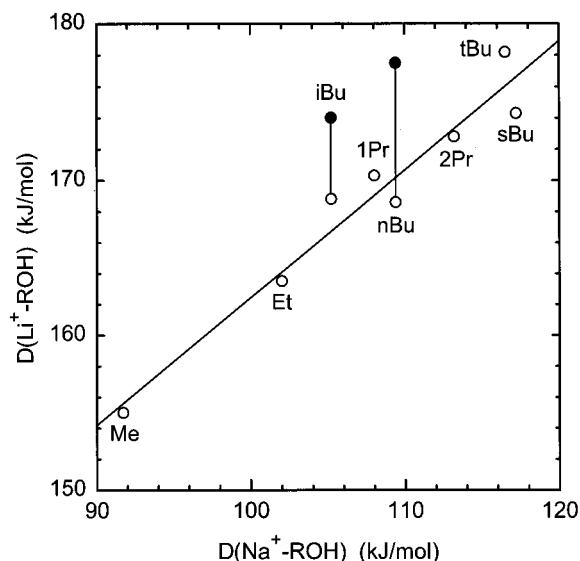


Figure 5. Open circles show bond dissociation energies at 0 K (in kJ/mol) for Na^+-ROH vs Li^+-ROH (taken from ref 2) where ROH = methanol (Me), ethanol (Et), 1-propanol (1Pr), 2-propanol (2Pr), *n*-butyl alcohol (nBu), isobutyl alcohol (iBu), sec-butyl alcohol (sBu), and *tert*-butyl alcohol (tBu). Closed circles show alternative values for Li^+ bound to *n*-butyl alcohol and isobutyl alcohol as discussed in the text.

polarizability of the ligands with increasing size. Clearly, there are other effects operating, however, as there is a 11 kJ/mol variation in the butanol binding energies even though their polarizabilities and dipole moments should be approximately equal. In part, these variations are a result of the additional complexation of the alkyl part of the alcohol to Na^+ . Such secondary complexation varies with the length of the alkyl chain and is not parametrized by average molecular quantities such as polarizability and dipole moment. Further, we find that the secondary and tertiary alcohols bind to Na^+ more tightly than the comparable primary alcohols, such that 2-propanol binds more tightly than *n*-butyl alcohol and isobutyl alcohol, even though the polarizabilities of the butanols are greater than that for 2-propanol. As the distinction between primary vs secondary and tertiary alcohols is realized for even the smallest complexes, it does not appear to be related to the lifetime corrections. Further, the experimental protocol for acquiring and analyzing the data for the various complexes is identical, such that this systematic difference in bond energies is unlikely to be attributable to experimental artifacts. Qualitatively, the stronger binding of the secondary and tertiary alcohols suggests that there are favorable inductive effects when more alkyl groups are attached to the carbon adjacent to the oxygen atom. However, this conclusion is mediated by the uncertainty in the precise relative values introduced in the next section.

Comparison to Lithium Ion Binding Affinities. The present collision-induced dissociation results are compared with thermochemistry obtained from similar CID studies of the $\text{Li}^+(\text{ROH})$ complexes in Figure 5.² We find excellent agreement in the trends observed in the relative bond energies. Clearly, the lithium ion affinities exceed those for sodium because the smaller ion has a shorter metal–ligand bond leading to a stronger electrostatic interaction. However, recent studies of the competitive dissociation of $\text{Li}^+(\text{R}_1\text{OH})(\text{R}_2\text{OH})$ complexes indicates that the bond energy determined by direct CID is slightly low for $\text{Li}^+(\text{n-BuOH})$.⁴ This work indicates that the lithium ion affinity for *n*-butyl alcohol should be 177.5 ± 8 kJ/mol, compared to 168.6 ± 8.2 kJ/mol determined in the earlier direct CID studies. Relative bond energies for other complexes (ROH = methanol,

ethanol, 1-propanol, and 2-propanol) are in excellent agreement in both studies. This hypothesis is bolstered by ab initio calculations⁴⁵ on the Li⁺(ROH) complexes performed after our direct CID experimental study. Theory confirms our absolute values obtained by direct CID with an average deviation between experiment and theory of 3 kJ/mol. However, the theoretical bond energy for Li⁺(*n*-BuOH) is the only system (out of eight) where theory is *above* our experimental result, strongly suggesting that the latter should be revised upward.

On the basis of ICR studies⁴⁶ of the relative binding affinities of Li⁺ to *n*-butyl alcohol ($E_{\text{rel}} = 0.0$ kJ/mol), isobutyl alcohol ($E_{\text{rel}} = -3.5$ kJ/mol), and sec-butyl alcohol ($E_{\text{rel}} = -2.3$ kJ/mol),⁴⁷ it is also possible that the Li⁺(*i*-BuOH) value measured by direct CID studies (168.8 ± 7.6 kJ/mol) is slightly low and should be about 174 ± 8 kJ/mol. (Theory⁴⁵ gives the relative energetics of these complexes as 0.0, -6.5 , and -6.1 kJ/mol, respectively, which suggest that the value for isobutyl alcohol should be 171 – 174 kJ/mol.) These higher values for the Li⁺(*n*-BuOH) and Li⁺(*i*-BuOH) complexes are included in Figure 5. On the basis of the correlation between the lithium and sodium cation affinities, this suggests that bond energies for Na⁺(*n*-BuOH) and Na⁺(*i*-BuOH) may also be somewhat low (by up to 9 kJ/mol).

It is unclear what problem might adversely affect the direct CID results for the alkali cation complexes with *n*-butyl alcohol and isobutyl alcohol but no other complexes. It occurred to us that systematically low bond energies could result from inadequate treatment in our data analysis of the internal rotations and torsions of these alcohols vs those in the metalated complexes. Therefore, we tried reanalyzing our data by treating all vibrational modes of the sodium cation complexes and the dissociation products having frequencies lower than 260 cm^{-1} as internal rotations. This leads to bond dissociation energies that are much lower than those reported in Table 1 for two reasons. The average internal energy of the complexes is less (because low frequency vibrations that can contain approximately kT of energy are replaced by rotors containing only $kT/2$) and there is a larger kinetic shift (because this treatment leads to two more internal rotors in the complexes compared to the alcohol products). Examination of the resultant entropies of activation shows that this treatment is comparable to the tight transition state limit previously investigated in several papers.^{1–3,26} In all cases, this tight transition state limit led to bond energies that were much too low compared with other available information. This suggests that this alternate treatment of the torsional modes of these complexes is not appropriate. Other rationales for low CID values of *n*-butyl alcohol and isobutyl alcohol but no other complexes are not apparent to us. It should be realized, however, that while such corrections may affect the precision of the relative sodium cation binding energies, the absolute binding energies measured here should still be accurate within the stated experimental uncertainties.

Comparison between Theory and Experiment. The sodium cation affinities of the alcohols at 0 K measured and calculated here are summarized in Table 3. The agreement between theory and experiment is good, as shown in Figure 6. The mean absolute deviation (MAD) between experiment and the MP2 theory values for the most stable conformers of all eight systems is 4.0 ± 3.4 kJ/mol, within the average experimental error of 4.7 ± 0.8 kJ/mol and well within expected computational accuracy. If we compare to the CBS-4 values, the MAD is 3.7 ± 3.3 kJ/mol, very similar to that for the MP2 values, while the CBS-Q values have a MAD from experiment of 3.3 ± 3.1 kJ/mol. We find that the four G2 bond energies have a MAD

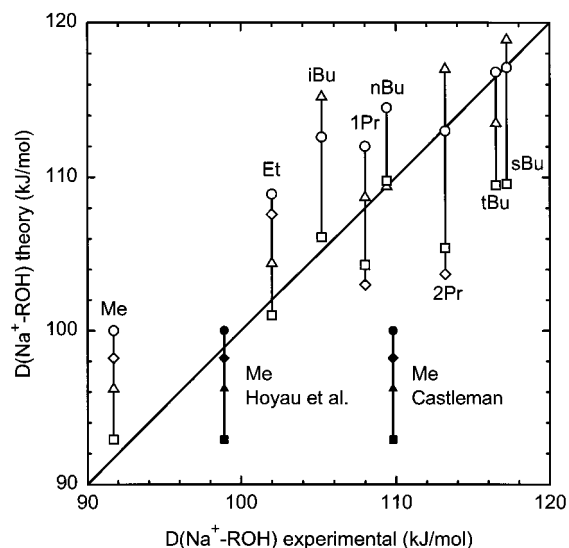


Figure 6. Ab initio calculated bond dissociation energies (in kJ/mol) for Na⁺–ROH where ROH = methanol (Me), ethanol (Et), 1-propanol (1Pr), 2-propanol (2Pr), *n*-butyl alcohol (nBu), isobutyl alcohol (iBu), sec-butyl alcohol (sBu), and *tert*-butyl alcohol (tBu) vs experimentally measured bond dissociation energies (in kJ/mol) taken from Table 4. All values are at 0 K. The various levels of theory shown are MP2 (○), G2 (◇), CBS-Q (△) and CBS-4 (□). The diagonal line indicates the values for which calculated and measured bond dissociation energies are equal. Solid symbols indicate experimental values for Na⁺(MeOH) taken from the literature and adjusted to 0 K: refs 34 (Hoyau et al.) and 49 (Castleman).

of 6.7 ± 2.0 kJ/mol. On the basis of the comparison with experimental results, none of these theories is obviously better than the others. Therefore, we believe that a reasonable estimate of the best theoretical bond energies are the median of all theoretical values with an anticipated error given by the range in these values, approximately ± 4 kJ/mol. The agreement between experiment and such median theoretical values is quite reasonable, with a MAD of 3.2 ± 1.5 kJ/mol.

In comparing the experimental and theoretical values, it should be realized that the comparisons above are restricted to theoretical values for the most stable conformation. Experimentally, it is possible that several of these conformers are formed in our flow tube source as kT at 298 K is 2.5 kJ/mol, comparable to the energy differences among the low-lying conformers (Table 3). As long as the barriers between the conformers are substantially larger than kT , which seems likely, then experimental formation of several conformers is feasible. Because of the extensive energy broadening introduced by the energy distributions of the reactants, the experiment is incapable of resolving the cross sections for such closely spaced conformers directly. However, the presence of such excited conformers could give experimental bond energies for the 1-propanol, *n*-butyl alcohol, isobutyl alcohol, and sec-butyl alcohol complexes that are a couple of kJ/mol weaker than those calculated for the ground state conformers, although such deviations are still within the experimental error cited. Bond energies for the methanol, ethanol, 2-propanol, and *tert*-butyl alcohol complexes are less likely to be affected by this complication.

Figure 6 shows that theoretical values for the primary alcohols are somewhat high compared to our experiments, while values for the secondary and tertiary alcohols are slightly low (but all are still within experimental or theoretical error). This effect can be quantified by noting that the experimental and MP2 theoretical values for the five primary alcohols exhibit a MAD of 6.3 ± 1.8 kJ/mol, while those for secondary and tertiary

TABLE 4: Enthalpies and Free Energies of Sodium Ion Binding of Na⁺-ROH at 0 and 298 K in kJ/mol^a

system	ΔH_0	$\Delta H_{298} - \Delta H_0^b$	ΔH_{298}	$T\Delta S_{298}^b$	ΔG_{298}
Na ⁺ (MeOH)	91.7(5.7)	1.5(0.2)	93.2(5.7)	27.5(0.5)	65.7(5.7)
Na ⁺ (EtOH)	102.0(3.7)	1.3(0.2)	103.3(3.7)	28.0(0.5)	75.3(3.7)
Na ⁺ (1-PrOH)	108.0(4.1)	1.3(0.2)	109.3(4.1)	28.9(0.6)	80.4(4.1)
Na ⁺ (2-PrOH)	113.2(4.3)	1.2(0.2)	114.4(4.3)	28.9(0.6)	85.5(4.3)
Na ⁺ (<i>n</i> -BuOH)	109.4(4.7)	0.9(0.2)	110.3(4.7)	28.1(0.5)	82.2(4.7)
Na ⁺ (<i>i</i> -BuOH)	105.2(5.7)	1.2(0.2)	106.4(5.7)	29.6(0.6)	76.8(5.7)
Na ⁺ (<i>s</i> -BuOH)	117.2(5.1)	1.2(0.2)	118.4(5.1)	30.0(0.6)	88.4(5.1)
Na ⁺ (<i>t</i> -BuOH)	116.5(4.1)	1.1(0.2)	117.6(4.1)	28.6(0.6)	89.0(4.1)

^a Uncertainties are listed in parentheses. ^b Calculated using standard formulas and molecular constants given in Tables 1S and 2S.

alcohols agree very well, with a MAD of only 0.1 ± 0.1 kJ/mol. For the CBS-4 calculations, the MAD from experimental values for the primary alcohols is 1.4 ± 1.3 kJ/mol, while the secondary and tertiary alcohols show a MAD of 7.5 ± 0.4 kJ/mol. Theory has mixed results in reproducing the experimentally observed enhancement in going from primary alcohols to secondary and tertiary alcohols. For instance, MP2, G2, and CBS-4 theories find that the 1- and 2-propanols have similar affinities for Na⁺ (a difference of only 1 kJ/mol) while CBS-Q finds an enhancement of 9.3 kJ/mol, compared to an experimental difference of 5.2 kJ/mol. While both MP2 and CBS-4 find that the most weakly bound butanol is isobutyl alcohol, in agreement with experiment (whether adjusted upward or not), CBS-Q theory finds that *n*-butyl alcohol has the weakest sodium cation affinity, while that for isobutyl alcohol is actually higher than that for *tert*-butyl alcohol. This result is difficult to understand when compared to the results obtained for the 1-propanol and 2-propanol systems. In agreement with experiment, all three levels of theory find that *sec*-butyl alcohol has the highest sodium cation affinity, but CBS-Q finds a lower affinity for *tert*-butyl alcohol, while MP2 and CBS-4 theories and experiment find a very similar affinity. Because theory does not provide a uniform prediction of the relative trends in the sodium cation affinities of the primary vs secondary and tertiary alcohols, theory cannot be used to definitively ascertain whether the present CID results for *n*-butyl alcohol and isobutyl alcohol might be slightly low relative to the other alcohols, as suggested by comparison with the measured lithium cation affinities. However, we note that increasing the sodium cation affinities for *n*-butyl alcohol and isobutyl alcohol would make the agreement between experiment and theory in these two systems more like that observed for the secondary and tertiary alcohols, but then less like that for all other primary alcohols.

Conversion to 298 K Values. To allow comparison to previous literature values and commonly used experimental conditions, we convert the 0 K bond energies determined here to 298 K bond enthalpies and free energies. The enthalpy conversions are calculated using standard formulas and the vibrational and rotational constants given in Tables 1S and 2S. Table 4 lists 0 and 298 K enthalpy, free energy, and enthalpic and entropic corrections for all systems experimentally determined.

Comparison with Literature Values. The only system included in the present work that has been studied extensively is Na⁺(MeOH). High-pressure mass spectrometry (HPMS) measurements by Castleman and co-workers⁴⁹ yield a 298 K enthalpy of 111.3 kJ/mol (109.8 kJ/mol at 0 K) while the recent HPMS work of Hoyau et al. yields 100.4 ± 0.8 kJ/mol (98.9 kJ/mol at 0 K).³⁴ Our experimental value of 93.2 ± 5.7 kJ/mol agrees reasonably well with the most recent HPMS experimental value but falls well below the value of Castleman and co-workers (Figure 6). Hoyau et al. note that the sodium cation affinities measured by the Castleman group are consistently higher than other values in the literature.

The good agreement between the MP2 and G2 theories and the value of Hoyau et al. make a tempting argument that the Na⁺ bond energy to methanol is about 99 kJ/mol at 0 K. However, after a careful analysis of our data, we could find no experimental artifacts or alternate data analysis strategies that could yield a CID threshold more consistent with this value. We note that the value from CBS-Q theory (arguably the most accurate theoretical approach used here) falls near midway between our experimental value and that of Hoyau et al. and is well within our experimental uncertainty. It is certainly plausible that the Na⁺(MeOH) bond energy is most precisely assigned toward the upper end of our experimental error.

Previous results from calculations on the Na⁺(MeOH) complex include 298 K enthalpies of 112.1 kJ/mol from Feng and Gronert (MP2/6-31+G*),⁵⁰ 100.0 kJ/mol from Remko and Sarisky (G2 theory),⁵¹ and 101.3 kJ/mol from Hoyau et al. (MP2-(full)/6-311+G(2d,2p)//MP2(full)6-31G* including BSSE).³⁴ The latter two calculations are reproduced in the present work. The value from Feng and Gronert appears to be too high because of the smaller basis set used and because BSSE (which we calculate is 4.8 kJ/mol with a larger basis set) is not included in their value.

The only other experimental value available for the sodium cation alcohol affinities is for 2-propanol as measured using the kinetic method by Feng and Gronert.⁵⁰ Their value of 124.3 kJ/mol has been anchored to measurements for acetone and amides and so does not follow the usual kinetic method protocol of dealing with reference compounds of the same functional group. The acetone value used as a reference is taken from work of Castleman and co-workers,⁴⁹ a value that is higher than recent measurements by Hoyau et al.³⁴ (by 11.8 ± 2.2 kJ/mol) and our group⁵² (by 9.2 ± 4.2 kJ/mol). This clearly can explain why their value is about 10 kJ/mol larger than the 298 K binding enthalpy of 114.4 ± 4.3 kJ/mol measured here. Calculations (MP2/6-31G*) by this group for sodium binding affinities of ethanol and 2-propanol are 117.1 and 120.5 kJ/mol. For the methanol, ethanol, and 2-propanol systems, their calculations are systematically higher than our MP2/6-311+G(2d,2p) values by 8 ± 2 kJ/mol and higher than our CBS-4 results by 15 ± 2 kJ/mol, again because of the smaller basis set and neglect of BSSE.

Conclusions

The kinetic energy dependencies of the collision-induced dissociations of Na⁺(ROH), ROH = methanol, ethanol, 1-propanol, 2-propanol, *n*-butyl alcohol, isobutyl alcohol, *sec*-butyl alcohol, and *tert*-butyl alcohol, with Xe are examined in a guided ion beam mass spectrometer. The dominant dissociation process in all cases is formation of Na⁺ + ROH. Thresholds at 0 K for these processes are determined after consideration of the effects of reactant internal energy, multiple collisions with Xe, and lifetime effects using a phase space limit transition state model. Our experimental results for Na⁺(MeOH) agree reasonably well

with high-pressure mass spectrometry experiments of Hoyau et al.³⁴ but not with those of Castleman and co-workers.⁴⁹ Likewise, the experimental value from Feng and Gronert⁵⁰ for Na⁺(2-PrOH) determined using the kinetic method is well outside of our experimental errors. Values reported here for the other six alcohols constitute the first experimental determinations of the sodium cation binding affinities. Comparisons of our experimental values with recent work on analogous lithium cation–alcohol complexes² show similar trends but suggest that the relative values for *n*-butyl alcohol and isobutyl alcohol might be somewhat low. Nevertheless, the absolute values are still likely to be accurate within the experimental errors cited. This is confirmed by good agreement with ab initio calculations at several levels of theory. Theoretical results also indicate that several low-energy conformers could complicate the experimental results, but again this is unlikely to change the absolute values outside the experimental errors.

Supporting Information Available: Table 1S lists vibrational frequencies and average vibrational energies at 298 K of the neutral molecules and sodiated complexes determined from vibrational analyses at the MP2(full)/6-31G* level. Table 2S lists rotational constants for the energized molecule and transition state for all eight Na⁺(ROH) systems. A complete set of figures for all eight systems examined are shown in Figures 1S and 2S. This material is available free of charge via the Internet at <http://pubs.acs.org>.

Acknowledgment. Funding for this work was provided by the National Science Foundation under Grant CHE-9530412.

References and Notes

- Rodgers, M. T.; Armentrout, P. B. *J. Phys. Chem. A* **1997**, *101*, 1238.
- Rodgers, M. T.; Armentrout, P. B. *J. Phys. Chem. A* **1997**, *101*, 2614.
- Rodgers, M. T.; Ervin, K. M.; Armentrout, P. B. *J. Chem. Phys.* **1997**, *106*, 4499.
- Rodgers, M. T.; Armentrout, P. B. *J. Chem. Phys.* **1998**, *109*, 1787.
- Curtiss, L. A.; Raghavachari, K.; Trucks, G. W.; Pople, J. A. *J. Chem. Phys.* **1991**, *94*, 7221.
- Nyden, M. R.; Petersson, G. A. *J. Chem. Phys.* **1981**, *75*, 1843. Petersson, G. A.; Al-Laham, M. A. *J. Chem. Phys.* **1991**, *94*, 6081. Petersson, G. A.; Tensfeldt, T.; Montgomery, J. A. *J. Chem. Phys.* **1991**, *94*, 6091. Montgomery, J. A.; Ochterski, J. W.; Petersson, G. A. *J. Chem. Phys.* **1994**, *101*, 5900.
- Ochterski, J. W.; Petersson, G. A.; Montgomery, J. A. *J. Chem. Phys.* **1996**, *104*, 2598.
- Ervin, K. M.; Armentrout, P. B. *J. Chem. Phys.* **1985**, *83*, 166.
- Schultz, R. H.; Armentrout, P. B. *Int. J. Mass Spectrom. Ion Processes* **1991**, *107*, 29.
- Teloy, E.; Gerlich, D. *Chem. Phys.* **1974**, *4*, 417. Gerlich, D. Diplomarbeit, University of Freiburg, Federal Republic of Germany, 1971. Gerlich, D. In *State-Selected and State-to-State Ion–Molecule Reaction Dynamics, Part I, Experiment*, Ng, C.-Y., Baer, M., Eds.; *Adv. Chem. Phys.* **1992**, *82*, 1.
- Aristov, N.; Armentrout, P. B. *J. Phys. Chem.* **1986**, *90*, 5135.
- Hales, D. A.; Armentrout, P. B. *J. Cluster Sci.* **1990**, *1*, 127.
- Armentrout, P. B. In *Advances in Gas-Phase Ion Chemistry*; Adams, N. G., Babcock, L. M., Eds.; JAI: Greenwich, 1992; Vol. 1, pp 83–119.
- Dalleska, N. F.; Honma, K.; Sunderlin, L. S.; Armentrout, P. B. *J. Am. Chem. Soc.* **1994**, *116*, 3519.
- Schultz, R. H.; Crellin, K. C.; Armentrout, P. B. *J. Am. Chem. Soc.* **1992**, *113*, 8590.
- Dalleska, N. F.; Honma, K.; Armentrout, P. B. *J. Am. Chem. Soc.* **1993**, *115*, 12125.
- Khan, F. A.; Clemmer, D. C.; Schultz, R. H.; Armentrout, P. B. *J. Phys. Chem.* **1993**, *97*, 7978.
- Schultz, R. H.; Armentrout, P. B. *J. Chem. Phys.* **1992**, *96*, 1046.
- Fisher, E. R.; Kickel, B. L.; Armentrout, P. B. *J. Phys. Chem.* **1993**, *97*, 10204.
- Fisher, E. R.; Kickel, B. L.; Armentrout, P. B. *J. Chem. Phys.* **1992**, *97*, 4859.
- Beyer, T. S.; Swinehart, D. F. *Comm. Assoc. Comput. Machines* **1973**, *16*, 379. Stein, S. E.; Rabinovitch, B. S. *J. Chem. Phys.* **1973**, *58*, 2438. *Chem. Phys. Lett.* **1977**, *49*, 1883.
- Pople, J. A.; Schlegel, H. B.; Raghavachari, K.; DeFrees, D. J.; Binkley, J. F.; Frisch, M. J.; Whitesides, R. F.; Hout, R. F.; Hehre, W. J. *Int. J. Quantum Chem. Symp.* **1981**, *15*, 269. DeFrees, D. J.; McLean, A. D. *J. Chem. Phys.* **1985**, *82*, 333.
- Waage, E. V.; Rabinovitch, B. S. *Chem. Rev.* **1970**, *70*, 377.
- Chesnavich, W. J.; Bowers, M. T. *J. Phys. Chem.* **1979**, *83*, 900.
- See, for example: Sunderlin, L. S.; Armentrout, P. B. *Int. J. Mass Spectrom. Ion Processes* **1989**, *94*, 149.
- More, M. B.; Glendening, E. D.; Ray, D.; Feller, D.; Armentrout, P. B. *J. Phys. Chem.* **1996**, *100*, 1605. Ray, D.; Feller, D.; More, M. B.; Glendening, E. D.; Armentrout, P. B. *J. Phys. Chem.* **1996**, *100*, 16116. More, M. B.; Ray, D.; Armentrout, P. B. *J. Phys. Chem. A* **1997**, *101*, 831.
- See for example, Figure 1 in ref 16.
- Armentrout, P. B.; Simons, J. *J. Am. Chem. Soc.* **1992**, *114*, 8627.
- Hyperchem Computational Chemistry Software Package, Version 5.0, Hypercube Inc., Tallahassee, FL; 1996.
- Frisch, M. J.; Trucks, G. W.; Schlegel, H. B.; Scuseria, G. E.; Robb, M. A.; Cheeseman, J. R.; Zakrzewski, V. G.; Montgomery, J. A., Jr.; Stratmann, R. E.; Burant, J. C.; Dapprich, S.; Millam, J. M.; Daniels, A. D.; Kudin, K. N.; Strain, M. C.; Farkas, O.; Tomasi, J.; Barone, V.; Cossi, M.; Cammi, R.; Mennucci, B.; Pomelli, C.; Adamo, C.; Clifford, S.; Ochterski, J.; Petersson, G. A.; Ayala, P. Y.; Cui, Q.; Morokuma, K.; Malick, D. K.; Rabuck, A. D.; Raghavachari, K.; Foresman, J. B.; Cioslowski, J.; Ortiz, J. V.; Stefanov, B. B.; Liu, G.; Liashenko, A.; Piskorz, P.; Komaromi, I.; Gomperts, R.; Martin, R. L.; Fox, D. J.; Keith, T.; Al-Laham, M. A.; Peng, C. Y.; Nanayakkara, A.; Gonzalez, C.; Challacombe, M.; Gill, P. M. W.; Johnson, B.; Chen, W.; Wong, M. W.; Andres, J. L.; Gonzalez, C.; Head-Gordon, M.; Replogle, E. S.; Pople, J. A. *Gaussian 98, Revision A.3*; Gaussian, Inc.: Pittsburgh, PA, 1998.
- Møller, C.; Plesset, M. S. *Phys. Rev.* **1934**, *46*, 618.
- Bartlett, R. J. *Annu. Rev. Phys. Chem.* **1981**, *32*, 359.
- Hehre, W. J.; Radom, L.; Schleyer, P. v. R.; Pople, J. A. *Ab initio Molecular Orbital Theory*; Wiley: New York, 1986.
- Hoyau, S.; Norrman, K.; McMahon, T. B.; Ohanessian, G. *J. Am. Chem. Soc.*, in press.
- Exploring Chemistry with Electronic Structure Methods*, 2nd ed.; Foresman, J. B.; Frisch, A.; Gaussian: Pittsburgh, 1996.
- Fogarasi, G.; Pulay, P. In *Vibrational Spectra and Structure*; J. R. Durig, Ed.; Elsevier: New York, 1985; Vol. 14, p 125.
- Boys, S. F.; Bernardi, R. *Mol. Phys.* **1970**, *19*, 553.
- Van Duijneveldt, F. B.; van Duijneveldt-van de Rijdt, J. G. C. M.; van Lenthe, J. H. *Chem. Rev.* **1994**, *94*, 1873.
- Hill, S. E.; Glendening, E. D.; Feller, D. *J. Phys. Chem. A* **1997**, *101*, 6125. Hill, S. E.; Feller, D.; Glendening, E. D. *J. Phys. Chem. A* **1998**, *102*, 3813.
- Nicholas, J. B.; Hay, B. P.; Dixon, D. A. *J. Phys. Chem.* **1999**, *103*, 1394.
- In three cases (ROH = MeOH, *i*-BuOH, and *s*-BuOH), very small amounts of other products with masses consistent with hydrocarbon cations were also observed. It is believed that these peaks probably are formed from decomposition of very small amounts of contaminant hydrocarbon polymer cations formed in the flow tube source.
- Meyer, F.; Khan, F. A.; Armentrout, P. B. *J. Am. Chem. Soc.* **1995**, *117*, 9740.
- Lifshitz, C. *Adv. Mass Spectrom.* **1989**, *11*, 113.
- CRC Handbook of Chemistry and Physics*; Weast, R. C., Astle, M. J., Eds.; CRC Press: Boca Raton, FL, 1982.
- Siu, F. M.; Ma, N. L.; Tsang, C. W. *Chem. Phys. Lett.* **1998**, *288*, 408.
- Taft, R. W.; Anvia, F.; Gal, J.-F.; Walsh, S.; Capon, M.; Holmes, M. C.; Hosn, K.; Oloumi, G.; Vasanwala, R.; Yazdani, S. *Pure Appl. Chem.* **1990**, *62*, 17.
- These 0 K relative energies are corrected from the original free energies at 373 K, ΔG_{373} , taken from ref 46 using information compiled in ref 2.
- More, M. B.; Ray, D.; Armentrout, P. B. *J. Phys. Chem. A* **1997**, *101*, 4254; More, M. B.; Ray, D.; Armentrout, P. B. *J. Phys. Chem. A* **1997**, *101*, 7007.
- Guo, B. C.; Conklin, B. J.; Castleman, A. W. *J. Am. Chem. Soc.* **1989**, *111*, 6506.
- Feng, W. Y.; Gronert, S. Personal communication.
- Remko, M.; Sarisky, M. *Chem. Phys. Lett.* **1998**, *282*, 227. These authors report G2 energies yielding a 298 K bond enthalpy of 0.0380950 h which they convert to 24.5 kcal/mol (102.5 kJ/mol). Our G2 calculation reproduces the number in hartrees precisely. Using the conversion factors 1 h = 27.2114 and 1 eV = 23.06054 kcal/mol, this calculated value is actually 23.9 kcal/mol (100.0 kJ/mol). All of the computed values in Tables 3 and 4 of their work appear to be inaccurately converted.
- Armentrout, P. B.; Rodgers, M. T. *J. Phys. Chem. A*, submitted for publication.